Array-enhanced coherence resonance in the diffusively coupled active rotators and its analysis with the nonlinear Fokker-Planck equation

Takashi Kanamaru and Masatoshi Sekine

September 12, 2003

Abstract

The array-enhanced coherence resonance (AECR) in the diffusively coupled active rotators is investigated and its analysis with the nonlinear Fokker-Planck equation is presented. By considering the nonlinear Fokker-Planck equation of the rotators, it is found that the time-periodic solution exists in some parameter range. By solving the equation of a rotator and the Fokker-Planck equation simultaneously, the behavior of a rotator in the system with infinite number of rotators is considered, and it is found that AECR also takes place in this infinite system. Thus it is concluded that AECR is caused by the time-periodic solution of the probability density induced by noise.

IEICE Transactions on Fundamentals, vol.E86-A, no.9, (2003) 2197-2202.

1 Introduction

In noisy nonlinear systems, stochastic resonance (SR) is a well-known phenomenon where a weak periodic signal is enhanced by its background noise and observed in many systems, such as bistable ring lasers, semiconductor devices, chemical reactions, and neural systems[1]. When a periodic signal and noise are injected to such systems simultaneously, the signal to noise ratio of the output signal is maximized at an optimal noise intensity.

Even when the periodic input does not exist, it is known that the coherence, or, typically the periodicity of the output of the system is maximized at an optimal noise intensity in some nonlinear systems, and this phenomenon is called coherence resonance (CR)[2]. CR is often demonstrated with the neuronal model, *e.g.*, the Hodgkin-Huxley model[3] and the FitzHugh-Nagumo model[4]. As a neural model, CR in the spatially extended systems, or, the neuronal network is of importance. In Refs. [5, 6, 7], the diffusively coupled FitzHugh-Nagumo models is treated, and it is observed that the maximum of the coherence of the system is further enhanced by the coupling. This phenomenon is called the array-enhanced coherence resonance (AECR). The diffusive connections correspond to the electrical coupling with gap junctions[8] in the neuronal system. Usually, the synaptic, or, the chemical couplings are thought to be more typical in the brain than the electrical ones, but recently the importance of the electrical couplings is emphasized by several authors[9, 10, 11]. Thus AECR might be a source of the oscillation in the biological system.

In the present paper, the array-enhanced coherence resonance in the diffusively coupled active rotators are treated and its analysis with the nonlinear Fokker-Planck equation is presented. In Sect. 2, the diffusively coupled active rotators with noise are defined and AECR is observed by numerical simulations. In Sect. 3, the nonlinear Fokker-Planck equation is introduced and its bifurcation diagram is presented. It is found that the time-periodic solution exists in some parameter range. By solving the equation of a rotator and the Fokker-Planck equation simultaneously, the behavior of the rotator in the system with infinite number of rotators is considered, and it is found that AECR also takes place in this infinite system. Conclusions and discussions are presented in the final section.

2 Array-enhanced coherence resonance in the diffusively coupled active rotators

Let us consider the diffusively coupled active rotators with noise[12, 13, 14, 15] written as

$$\dot{\theta}_i = 1 - a\sin\theta_i + \frac{g}{N}\sum_{j=1}^{N}\sin(\theta_j - \theta_i) + \xi_i(t), \tag{1}$$

$$\langle \xi_i(t)\xi_j(t')\rangle = D\delta_{ij}\delta(t-t'), \tag{2}$$

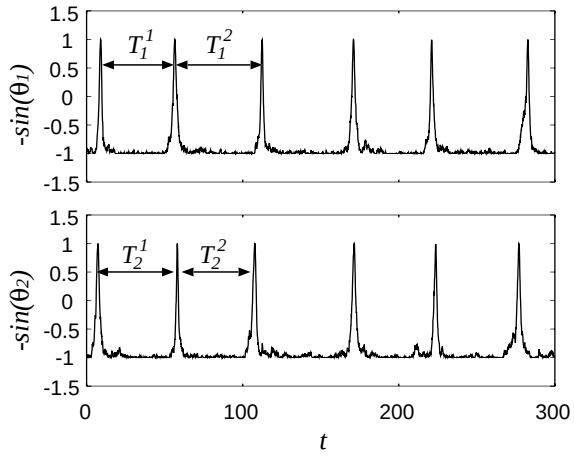

Figure 1: The time series of $-\sin(\theta_1)$ and $-\sin(\theta_2)$ for $D = 0.03$ and $g = 0.5$.

where a is a system parameter, g is the coupling strength, N is the number of rotators, $\xi_i(t)$ is Gaussian white noise, D is the noise intensity, and δ_{ij} denotes Kronecker's delta. This model is first treated by Shinomoto and Kuramoto[12], and we use the same one in the following with some modifications of the parameters. For $a < 1$, the active rotator oscillates, and for $a > 1$, it shows the typical behavior of the excitable system, namely, it has a stable equilibrium and $-\sin(\theta_i)$ shows a pulse-like waveform with an appropriate amount of disturbance. The neurons which compose the neuronal network in the brain are the typical examples of the excitable system, thus the active rotator can be regarded as a model of a single neuron, and their diffusive connections correspond to the electrical coupling with gap junctions[8]. Moreover, the active rotator can also be regarded as a model of the average behavior of some ensemble of neurons. In the following, the parameter is fixed as $a = 1.01$. The time series $-\sin(\theta_1)$ and $-\sin(\theta_2)$ for $D = 0.03$ and $g = 0.5$ are shown in Fig. 1. To integrate Eq. (1) numerically, the second order Runge-Kutta method[16] is used.

Let us define the firing time of the i-th rotator as the time when $-\sin(\theta_i)$ exceeds the value 0.5, and define the k-th firing time of the i-th rotator as t_i^k. With t_i^k, the interspike interval of the i-th rotator is defined as

$$T_i^k = t_i^{k+1} - t_i^k, \tag{3}$$

and, with T_i^k, the coherence measure[5] R is defined as

$$R = \langle R_i \rangle_i \equiv \left\langle \frac{\langle T_i^k \rangle_k}{\sqrt{\langle (T_i^k)^2 \rangle_k - \langle T_i^k \rangle_k^2}} \right\rangle_i , \tag{4}$$

where $\langle \cdot \rangle_k$ denotes the average over the firing number k, and $\langle \cdot \rangle_i$ denotes the average over the rotators $1 \le i \le N$. For periodic pulse trains, R takes a large value, and, for highly random pulse trains, it takes a small value. For example, R diverges for purely periodic pulse trains, and it takes the value 1 for pulse trains generated by the Poisson process. Note that R_i is the reciprocal of the coefficient of variation which is often used to measure the randomness of a spike train in the neuroscience[17].

To measure the degree of synchronization, let us define S as

$$S = \langle S(t) \rangle_t, \tag{5}$$

$$S(t) = \langle \cos(\theta_i - \theta_{i'}) \rangle_{i \neq i'} . \tag{6}$$

If the rotators represent the neuronal models, the correlation C of the firings of each rotator is also important. To define C, the time under observation is divided into n bins of the width Δ, and the number of firings in the l-th bin is denoted as X_l and Y_l for two time series $-\sin(\theta_i)$ and $-\sin(\theta_j)$. Note that the width Δ is sufficiently small so that X_l and Y_l take the value 0 or 1. Then $X = \sum X_l$ and $Y = \sum Y_l$ are the numbers of firings, and $Z = \sum X_l Y_l$ is the number of coincident firings. The correlation coefficient C between two pulse trains[18] is defined as

$$C = \frac{Z - (XY)/n}{\sqrt{X(1 - X/n)Y(1 - Y/n)}} \in [-1, 1]. \tag{7}$$

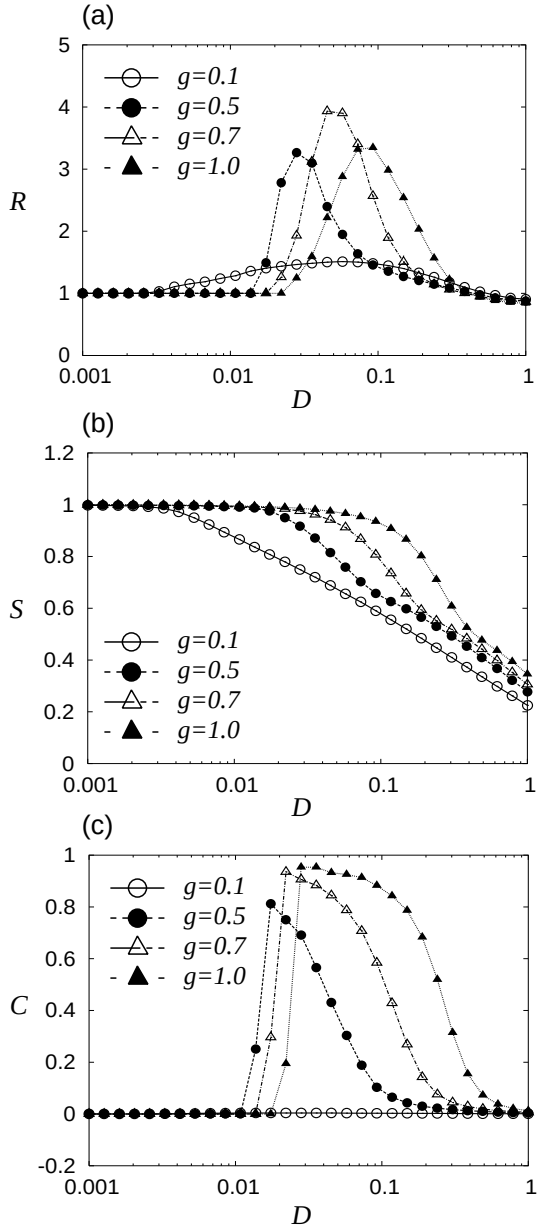

Figure 2: The dependences of (a) R, (b) S, and (c) C on the noise intensity D for $g = 0.1$, 0.5, 0.7, and 1.0 with $N = 100$.

Note that C takes the value 1 for the identical pulse trains and takes the value 0 in the large n limit for two pulse trains without correlation. And C takes the value -1 when two pulse trains have a negative correlation, namely, $X_l + Y_l = 1$ for $l = 0, 1, 2, \cdots$. In the following, the value $\Delta = 5$ is used.

The dependences of R, S, and C on the noise intensity D for the system with $N = 100$ is shown in Fig. 2. As shown in Fig. 2(a), for each value of g, R is maximized at an optimal noise intensity. This phenomenon shows that the periodicity of the firings of each rotator, or, the coherence is maximized at an optimal noise intensity and it is called coherence resonance (CR)[2]. Let us define the maximum value of R for each g as R_{peak}. It is observed that R_{peak} is also maximized at some value of g. The dependence of R_{peak} on the coupling strength g is shown in Fig. 3(a), and the maximization of R_{peak} is observed. This result shows that the degree of coherence is enhanced by the coupling of the rotators, and it is called array-enhanced coherence resonance (AECR)[5, 6, 7].

The dependence of S on the noise intensity D is shown in Fig. 2(b), and it shows that S monotonically decreases as D increases. This is because S takes large value even when the rotators fluctuate around the equilibrium points. If the rotator is regarded as a model of the neuron, the correlation C of the firings seems to be more important.

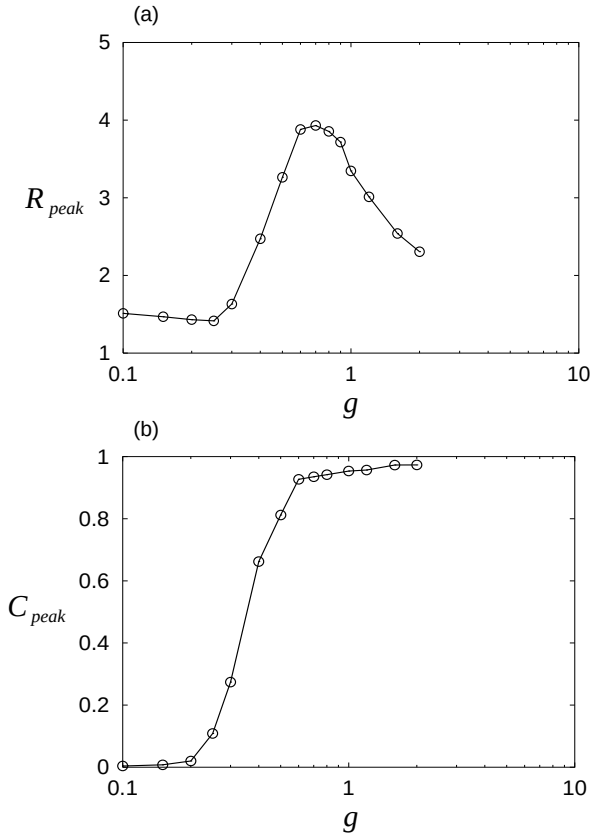

Figure 3: The dependences of (a) R_{peak} and (b) C_{peak} on the coupling strength g for $N = 100$.

The dependence of C on D is shown in Fig. 2(c), and it shows that C is also maximized as a function of D. This phenomenon is similar to so-called correlation resonance[19]. The dependence of the peak value C_{peak} of C on the coupling strength g is shown in Fig. 3(b), and it is observed that the C_{peak} monotonically increases with the increase of g. It is because all the rotators synchronize each other for large g. As shown in Figs. 2 and 3, the firings induced by AECR have the high coherence and the high correlation.

In the following sections, the mechanism of AECR in the diffusively coupled active rotators is investigated.

3 The analysis with the nonlinear Fokker-Planck equation

In this section, the system in the limit of $N \to \infty$ is considered. The analyses in this section correspond to those of asymmetric model treated by Sakaguchi *et al.*[13]. Let us consider the normalized number density of the rotator having the phase θ at time t written as

$$n(\theta, t) \equiv \frac{1}{N} \sum_{i=1}^{N} \delta(\theta_i - \theta). \tag{8}$$

With $n(\theta, t)$, Eq. (1) is rewritten as

$$\begin{aligned} \dot{\theta_i} &= 1 - a \sin\theta_i + \xi_i(t) \\ &\quad + g \int_0^{2\pi} d\theta' \sin(\theta' - \theta_i) n(\theta', t). \end{aligned} \tag{9}$$

In the limit of $N \to \infty$, $n(\theta, t)$ may be identified with the probability density, and in this approximation $n(\theta, t)$ follows the nonlinear Fokker-Planck equation [12, 13, 15, 20] written as

$$\begin{aligned} \frac{\partial n}{\partial t} &= -\frac{\partial}{\partial \theta}\{F(\theta, t) n\} + \frac{D}{2} \frac{\partial^2 n}{\partial \theta^2}, \\ F(\theta, t) &= 1 - a \sin\theta \end{aligned} \tag{10}$$

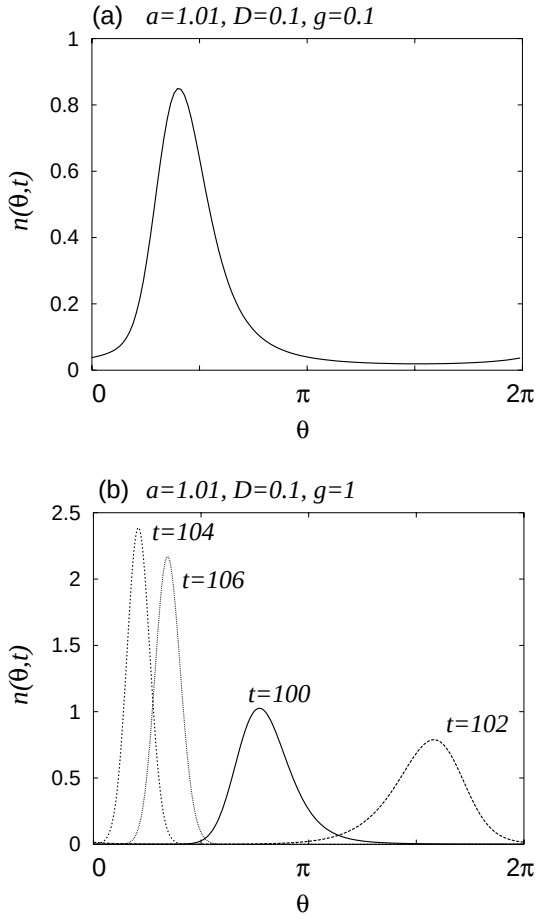

Figure 4: Numerical solutions of $n(\theta, t)$ for (a) $D = 0.1$ and $g = 0.1$ and for (b) $D = 0.1$ and $g = 1$.

$$+g \int_0^{2\pi} d\theta' \sin(\theta' - \theta) n(\theta', t). \tag{11}$$

First, let us consider the dependence of $n(\theta, t)$ on the coupling strength g and the noise intensity D. To obtain the numerical solution, Eq. (10) is transformed into a set of ordinary differential equations $\dot{\boldsymbol{x}} = \boldsymbol{f}(\boldsymbol{x})$ for the spatial Fourier coefficients of $n(\theta, t)$, and they are numerically integrated with the fourth order Runge-Kutta method. The numerical solutions of Eq. (10) for $D = 0.1$ and $g = 0.1$ and for $D = 0.1$ and $g = 1$ are shown in Figs. 4(a) and (b), respectively. It is found that Eq. (10) typically has the stationary density (S) and the time-periodic density (P) according to the values of g and D as shown in Figs. 4(a) and (b), respectively. When the system converges to the stationary density S, all the rotators fluctuate around their equilibria or they fire without correlation, and when it converges to the time-periodic density P, the rotators oscillate periodically with some degree of correlations.

A bifurcation diagram in the (D, g) plane is shown in Fig. 5. This result seems to agree with that of Sakaguchi *et al.*[13]. The open circles show the parameters where the numerically obtained $n(\theta, t)$ converges to the time-periodic density, and the solid and dotted lines are the Hopf bifurcation line and the saddle-node bifurcation line, respectively. Two saddle-node bifurcation lines intersect at a cusp bifurcation point, and a saddle-node bifurcation line, a Hopf bifurcation line, and a saddle separatrix loop bifurcation line (not shown) intersect at a Bogdanov-Takens bifurcation point[21, 22]. The Hopf and saddle-node bifurcation lines are obtained as follows. We consider a set of ordinary differential equations $\dot{\boldsymbol{x}} = \boldsymbol{f}(\boldsymbol{x})$ for the spatial Fourier coefficients of $n(\theta, t)$, and the stationary solution $\boldsymbol{x}_0$ which satisfies $\boldsymbol{f}(\boldsymbol{x}_0) = 0$ is numerically obtained. According to the numerically obtained eigenvalues of the Jacobian matrix $D\boldsymbol{f}(\boldsymbol{x}_0)$, the bifurcation lines are determined.

A schematic bifurcation diagram around the Bogdanov-Takens bifurcation point is shown in Fig. 6. Schematic diagrams of the typical trajectories projected onto a two-dimensional plane in each area are also illustrated. In Ref. [13], a low dimensional model of Eq. (10) is investigated and the theoretical analysis of these bifurcations are presented.

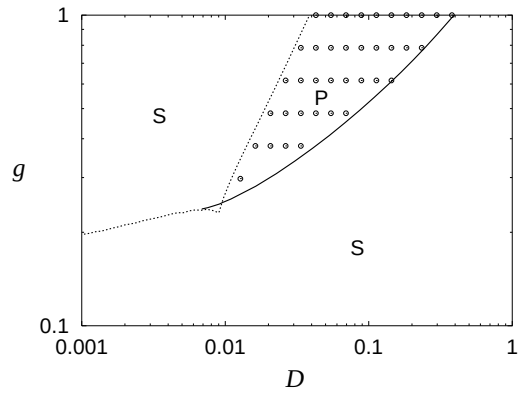

Figure 5: A bifurcation diagram in the (D, g) plane. The open circles show the parameters where the numerically obtained $n(\theta, t)$ converges to the time-periodic density, and the solid and dotted lines are the Hopf bifurcation line and the saddle-node bifurcation line, respectively.

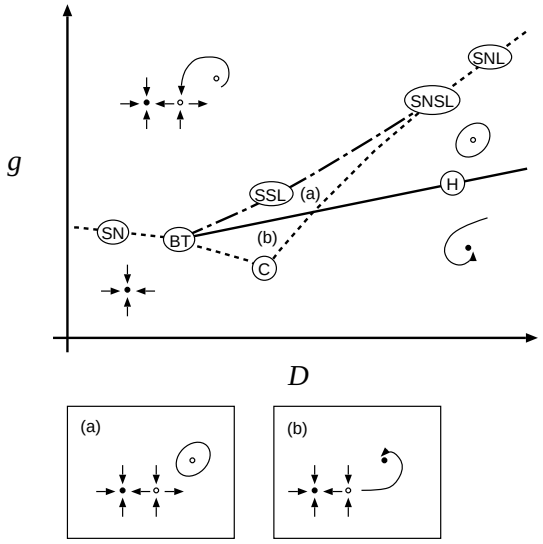

Figure 6: A schematic bifurcation diagram around the Bogdanov-Takens bifurcation point. The solid, dotted, and dash-dotted lines denote the Hopf bifurcation line, the saddle-node bifurcation line, and the saddle-separatrix loop bifurcation line, respectively. Schematic diagrams of the typical trajectories projected onto a two-dimensional plane in each area are also illustrated. The filled and open circles in the trajectories denote the stable and unstable equilibrium points, respectively. And the solid closed curve denotes the stable limit cycle. The meanings of the abbreviations are as follows: SN - saddle-node, H - Hopf, C - Cusp, BT - Bogdanov-Takens, SSL - saddle separatrix loop, SNSL - saddle-node separatrix loop, and SNL - saddle-node on limit cycle.

To compare the behavior of a rotator in the system for finite N with the behavior of the system in the limit of $N \to \infty$, let us consider the system governed by Eqs. (9) and (10) and we call it an infinite system in the following. The dependence of the coherence measure R of the infinite system also shows the typical property of CR, namely, it takes a maximum value at an optimal noise intensity. As shown in Fig. 7, R takes a maximum value when D crosses the saddle-node bifurcation line and enters the region where the time-periodic density P exists. It is naturally understood because the time-periodic density acts as a periodic input to the rotator. The dependence of R_{peak} on the coupling strength g in the infinite system is shown in Fig. 8. It is observed that AECR also takes place in the infinite system. The maximum of R_{peak} is given by the optimal values of D and g on the bifurcation line as follows. When g is increased from the small value along the right branch of the saddle-node bifurcation line, the effective noise intensity of the rotator is thought to decrease, thus the firings of the rotator become more coherent. However, when g is increased further, the noise intensity D which causes the saddle-node bifurcation also increases (see Fig. 5), thus the firings become less coherent and R_{peak} decreases.

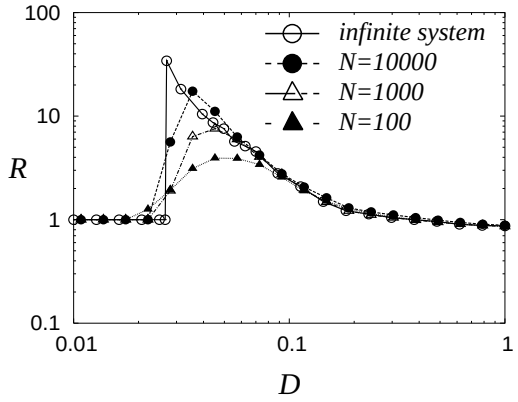

Figure 7: The dependences of R on D in the infinite system and the finite system with $N = 100$, 1000, and 10000 for $g = 0.7$.

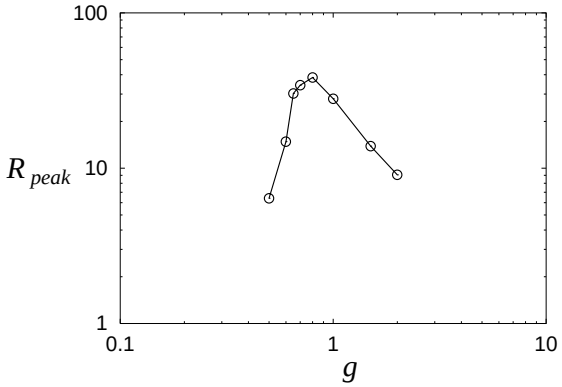

Figure 8: The dependence of R_{peak} on g for the infinite system.

From the above discussions, it is concluded that AECR in the diffusively coupled active rotators is caused by the time-periodic solution of the probability density of the rotators. When the array-enhancement takes place, the coupling term in Eq. (9) is dominant and acts as a periodic input in the dynamics of the rotator. On the other hand, for small g, *e.g.*, $g = 0.1$ in Fig. 2(a), there is no time-periodic density in the system (see Fig. 5), thus noise is dominant in Eq. (9) and the usual CR takes place.

The difference of the values of R_{peak}'s between Figs. 3(a) and 8 is caused by the finite size effect. The dependences of the coherence measure R on the noise intensity D of the infinite system and the finite system with $N = 100$, 1000, and 10000 for $g = 0.7$ are shown in Fig. 7. As N increases, the values of R for the finite system approach to those of the infinite system. Thus it can be concluded that the infinite system well describe the behavior of the finite system with large N.

4 Conclusions and discussions

The array-enhanced coherence resonance in the diffusively coupled active rotators with noise is investigated and its analysis with the nonlinear Fokker-Planck equation is presented.

When the noise intensity D is increased, the typical property of the coherence resonance (CR), namely, the maximization of the coherence measure R at an optimal noise intensity is observed. It is also found that the correlation C of the firings is maximized with the increase of D. Moreover, the further maximization of the maximum value R_{peak} of R with the increase of the coupling strength, known as array-enhanced coherence resonance (AECR), is observed.

By the analysis with the nonlinear Fokker-Planck equation, it is found that the probability density of the rotators with noise has a time-periodic solution in some parameter range. By solving the equation of the rotator and the Fokker-Planck equation simultaneously, the behavior of the rotator in the system with infinite number of

rotators is considered, and it is found that AECR also takes place in this infinite system. Thus it is concluded that AECR is caused by the time-periodic solution of the probability density of the rotators. On the other hand, for small g, there is no time-periodic density in the system (see Fig. 5), thus the usual CR takes place.

Acknowledgement

The author (T.K.) is grateful to Professor Takehiko Horita for his encouragement. This research was partially supported by a Grant-in-Aid for Encouragement of Young Scientists (B) (No. 14780260) from the Ministry of Education, Culture, Sports, Science, and Technology, Japan.

References

[1] L. Gammaitoni, P. Hänggi, P. Jung, and F. Marchesoni, "Stochastic resonance," Rev. Mod. Phys., vol.70, no.1, pp.223–287, 1998.

[2] A.S. Pikovsky and J. Kurths, "Coherence resonance in a noise-driven excitable system," Phys. Rev. Lett., vol.78, no.5, pp.775–778, 1997.

[3] S. Lee, A. Neiman, and S. Kim, "Coherence resonance in a Hodgkin-Huxley neuron," Phys. Rev. E, vol.57, no.3, pp.3292–3297, 1998.

[4] B. Lindner and L. Schimansky-Geier, "Analytical approach to the stochastic FitzHugh-Nagumo system and coherence resonance," Phys. Rev. E, vol.60, no.6, pp.7270–7276, 1999.

[5] B. Hu and C. Zhou, "Phase synchronization in coupled nonidentical excitable systems and array-enhanced coherence resonance," Phys. Rev. E, vol.61, no.2, pp.R1001–R1004, 2000.

[6] C. Zhou, J. Kurths, and B. Hu, "Array-enhanced coherence resonance: nontrivial effects of heterogeneity and spatial independence of noise," Phys. Rev. Lett., vol.87, no.9, pp.098101-1–098101-4, 2001.

[7] Y. Shinohara, T. Kanamaru, H. Suzuki, T. Horita, and K. Aihara, "Array-enhanced coherence resonance and forced dynamics in coupled FitzHugh-Nagumo neurons with noise," Phys. Rev. E, vol.65, no.5, pp.051906-1–051906-7, 2002.

[8] J.G. Nicholls, A.R. Martin, B.G. Wallace, and P. A. Fuchs, "From neuron to brain," Sinauer Associates Inc. Publishers, 2001.

[9] R.D. Traub, D. Schmitz, J.G.R. Jefferys, and A. Draguhn, "High-frequency population oscillations are predicted to occur in hippocampal pyramidal neuronal networks interconnected by axoaxonal gap junctions," Neurosci. vol.92, no.2, pp.407–426, 1999.

[10] M. Galarreta and S. Hestrin, "A network of fast-spiking cells in the neocortex connected by electrical synapse," Nature. vol.402, pp.72–75, 1999.

[11] J.R. Gibson, M. Beierlein, and B.W. Connors, "Two networks of electrically coupled inhibitory neurons in neocortex," Nature. vol.402, pp.75–79, 1999.

[12] S. Shinomoto and Y. Kuramoto, "Phase transitions in active rotator systems," Prog. Theor. Phys., vol.75, no.5, pp.1105–1110, 1986.

[13] H. Sakaguchi, S. Shinomoto, and Y. Kuramoto, "Phase transitions and their bifurcation analysis in a large population of active rotators with mean-field coupling," Prog. Theor. Phys., vol.79, no.3, pp.600–607, 1988.

[14] C. Kurrer and K. Schulten, "Noise-induced synchronous neuronal oscillations," Phys. Rev. E, vol.51, no.6, pp.6213–6218, 1995.

[15] S. Tanabe, T. Shimokawa, S. Sato, and K. Pakdaman, "Response of coupled noisy excitable systems to weak stimulation," Phys. Rev. E, vol.60, no.2, pp.2182–2185, 1999.

[16] J.R. Klauder and W.P. Petersen, "Numerical integration of multiplicative-noise stochastic differential equations," SIAM J. Numer. Anal., vol. 22, no.6, pp.1153–1166, 1985.

[17] W.R. Softky and C. Koch, "The highly irregular firing of cortical cells is inconsistent with temporal integration of random EPSPs," J. Neurosci., Vo.13, no.1 , pp.334–350, 1993.

[18] G. Palm, A.M.H.J. Aertsen, and G.L. Gerstein, "On the significance of correlations among neuronal spike trains," Biol. Cybern., vol.59, pp.1–11, 1988.

[19] H. Daido, "Correlation resonance in noise-driven coupled nonlinear oscillators," Physica D, vol.116, pp.325–341, 1998.

[20] Y. Kuramoto, "Chemical oscillations, waves, and turbulence," Springer, 1984.

[21] J. Guckenheimer and P. Holmes, "Nonlinear oscillations, dynamical systems, and bifurcations of vector fields," Springer, 1983.

[22] F.C. Hoppensteadt and E.M. Izhikevich, "Weakly connected neural networks," Springer, 1997.